



## Vertical Axis Wind Turbine Design Load Cases Investigation and Comparison with Horizontal Axis Wind Turbine

**Galinos, Christos; Larsen, Torben J.; Aagaard Madsen , Helge; Schmidt Paulsen, Uwe**

*Published in:*  
Energy Procedia

*Link to article, DOI:*  
[10.1016/j.egypro.2016.09.190](https://doi.org/10.1016/j.egypro.2016.09.190)

*Publication date:*  
2016

*Document Version*  
Publisher's PDF, also known as Version of record

[Link back to DTU Orbit](#)

*Citation (APA):*  
Galinos, C., Larsen, T. J., Aagaard Madsen , H., & Schmidt Paulsen, U. (2016). Vertical Axis Wind Turbine Design Load Cases Investigation and Comparison with Horizontal Axis Wind Turbine. *Energy Procedia*, 94, 319-328. <https://doi.org/10.1016/j.egypro.2016.09.190>

---

### General rights

Copyright and moral rights for the publications made accessible in the public portal are retained by the authors and/or other copyright owners and it is a condition of accessing publications that users recognise and abide by the legal requirements associated with these rights.

- Users may download and print one copy of any publication from the public portal for the purpose of private study or research.
- You may not further distribute the material or use it for any profit-making activity or commercial gain
- You may freely distribute the URL identifying the publication in the public portal

If you believe that this document breaches copyright please contact us providing details, and we will remove access to the work immediately and investigate your claim.



Available online at [www.sciencedirect.com](http://www.sciencedirect.com)

**ScienceDirect**

Energy Procedia 94 (2016) 319 – 328

Energy  
**Procedia**

13th Deep Sea Offshore Wind R&D Conference, EERA DeepWind'2016, 20-22 January 2016,  
Trondheim, Norway

## Vertical axis wind turbine design load cases investigation and comparison with horizontal axis wind turbine

Christos Galinos<sup>a,\*</sup>, Torben J. Larsen<sup>a</sup>, Helge A. Madsen<sup>a</sup>, Uwe S. Paulsen<sup>a</sup>

<sup>a</sup>Danish Technical University DTU Department of Wind Energy, Frederiksborgvej 399, Dk-4000 Roskilde, Denmark

---

### Abstract

The paper studies the applicability of the IEC 61400-1 ed.3, 2005 International Standard of wind turbine minimum design requirements in the case of an onshore Darrieus VAWT and compares the results of basic Design Load Cases (DLCs) with those of a 3-bladed HAWT. The study is based on aeroelastic computations using the HAWC2 aero-servo-elastic code. A 2-bladed 5 MW VAWT rotor is used based on a modified version of the DeepWind rotor. For the HAWT simulations the NREL 3-bladed 5 MW reference wind turbine model is utilized. Various DLCs are examined including normal power production, emergency shut down and parked situations, from cut-in to cut-out and extreme wind conditions. The ultimate and 1 Hz equivalent fatigue loads of the blade root and turbine base bottom are extracted and compared in order to give an insight of the load levels between the two concepts. According to the analysis the IEC 61400-1 ed.3 can be used to a large extent with proper interpretation of the DLCs and choice of parameters such as the hub-height. In addition, the design drivers for the VAWT appear to differ from the ones of the HAWT. Normal operation results in the highest tower bottom and blade root loads for the VAWT, where parked under storm situation (DLC 6.2) and extreme operating gust (DLC 2.3) are more severe for the HAWT. Turbine base bottom and blade root edgewise fatigue loads are much higher for the VAWT compared to the HAWT. The interpretation and simulation of DLC 6.2 for the VAWT lead to blade instabilities, while extreme wind shear and extreme wind direction change are not critical in terms of loading of the VAWT structure. Finally, the extreme operating gust wind condition simulations revealed that the emerging loads depend on the combination of the rotor orientation and the time stamp that the frontal passage of gust goes through the rotor plane.

© 2016 The Authors. Published by Elsevier Ltd. This is an open access article under the CC BY-NC-ND license (<http://creativecommons.org/licenses/by-nc-nd/4.0/>).

Peer-review under responsibility of SINTEF Energi AS

**Keywords:** VAWT; Darrieus; DLC; HAWT; onshore wind turbine

---

### 1. Introduction

Multi megawatt Vertical Axis Wind Turbine (VAWT) seem to be re-gaining a general interest in the wind energy sector as an alternative to Horizontal Axis Wind Turbine (HAWT). Current guidelines for certification of wind turbines as e.g. IEC 61400-1 ed.3 [1] covers any type of onshore wind turbine. However, as it has mainly been used for HAWTs during the development it is a bit uncertain whether the load-cases are also representative for VAWTs. This paper describes the results from the study on the applicability of the IEC 61400-1 ed.3 minimum design requirements in the

---

\* Corresponding author. Tel.: +45-46775033.  
E-mail address: [cgal@dtu.dk](mailto:cgal@dtu.dk)

case of an onshore Darrieus VAWT. It reveals potential critical design aspects of VAWT emerging from the Design Load Case (DLC) simulations. A comparison of basic DLCs is made between an equivalent rated power HAWT and the Darrieus wind turbine, as well. The study is based on aeroelastic simulations in time domain using the HAWC2 code [2], which has been validated for both HAWTs [11] and VAWTs [10,12,13].

## 2. Consideration about the definitions of the standard

The IEC 61400-1 ed.3 standard is applied on wind turbines without any distinction of the rotor type. A more accurate definition of the *hub height* is needed for VAWTs under investigation. The standard defines as *hub height* 'the height of the centre of the swept area of the wind turbine rotor above the terrain surface'. For VAWTs the location of the turbine's swept area centre changes under operation as a result of gravitational, centrifugal and aerodynamic forces this definition may not be so straight to use. This effect becomes significant in multi-megawatt Darrieus rotors where the blades are long and relatively flexible. In Fig. 2 on the left the VAWT rotor centreline is plotted at standing still and rated rotor speed. As it seen the height of the centre of the swept area changes. The *equator height* could also be used as equivalent *hub height* but becomes inconsistent in "V-rotor" or "Delta-rotor" VAWT configurations. In the present study the *hub height* is proposed and defined as 'the height of the centre of the rotor projected area of the wind turbine above the terrain surface when the turbine operates at nominal rotor speed'. This appears to be a definition usable for all types of VAWTs. Moreover, the rotor diameter is used in many equations of the standard and describes the transient wind conditions such as the extreme operating gust. It can be constant ("H-type" VAWT) or a function of height such as the Darrieus or "V-rotor" configurations. Thus, a representative value should be defined for different VAWT configurations. In this study the largest rotor diameter at nominal speed is used.

## 3. Wind Turbine models and simulation set up

The analysis is based on the DeepWind VAWT aeroelastic model [4] as it was modified to a 5 MW onshore version according to reference [7]. The blade aerodynamic profile and geometric characteristics were unchanged and only the blade cross section structure was modified in [7] to confine the large edgewise vibrations as reported in [4]. The actuator cylinder flow model implemented in HAWC2 [3] was employed together with the Stig Øye dynamic stall model [8] to capture the aerodynamics of the rotor.

In order to compare the load levels to a representative HAWT, the NREL 5 MW HAWT [5] was selected. HAWC2 was also utilized for the HAWT analysis, where the Blade Element Momentum model with the modified Beddoes-Leishmann dynamic stall model [9] captures the rotor aerodynamics. Multibody formulation and Timoshenko beam elements are used in the code to model the wind turbines structurally.

The HAWT rotor is variable speed with active blade pitch, while the VAWT is stall regulated and the variable speed is obtained using an inverter and an asynchronous generator model with slip of 0.8% [14]. The outputs that are reported from the VAWT simulations are the blade Bending Moments (BM), the turbine base bottom moments at the section where the blade is attached to the lower and upper part of, the blade deflection at equator station and the rotor torque and speed.

## 4. Investigated design load cases

IEC wind turbine class II was selected in the context of this study. The VAWT considered DLCs are summarized in Table 1 and described below. Extreme coherent gust with direction change wind condition (DLC 1.4), start up (DLC 3.x) and normal shut down (DLC 4.x) cases are highly dependent of the control strategy and are not investigated, as well as the DLCs 8.x for transport, assembly, maintenance and repair of the wind turbine. The wind conditions are set according to the standard except if otherwise stated. Turbulence category B ( $I_{ref} = 0.14 [-]$ ) is selected as the base scenario for Normal and Extreme Turbulence Models (NTM and ETM). Six turbulent seed realizations were simulated at every wind speed as proposed in the standard for robust statistical analysis and no further safety factors were applied in the presented results.

The ultimate loads coming of 50 year return period winds were calculated using the extrapolation of maximum values for normal operation of both turbines with NTM wind conditions (DLC 1.1).

The loads emerging from power production state under Extreme Wind Shear (EWS) and Extreme Wind Veer (EWV) transient conditions, both horizontal and vertical, DLC 1.5, are investigated for VAWT keeping the default transient time to 12 s.

The Extreme Operating Gust (EOG) event is considered without the combination of electrical system fault, even though it is proposed in the DLC 2.3 in order to investigate the net effect. The duration of the EOG is set to the default value of 10.5 s. In addition, the Taylor hypothesis is applied following the suggestion in [10] and the simulations are performed for different wind speeds and combinations of rotor orientation and front passage of the gust. The latter is done for the investigation of the gust frontal passage influence with respect to the blade position since the VAWT rotor extends in 3 dimensions. Another examined wind condition is the Extreme Direction Change (EDC) transient phenomenon which is used as a critical case during turbine start-up. In the present study the loads are evaluated when the VAWT is under normal power production and the EDC occurs. This can indicate how critical such an extreme case is.

For the emergency shut down scenario the turbine was equipped with a mechanical brake assuming that the electrical generator braking capability is out of order due to a failure. The brake torque is given by equation (1), where  $T_b^{max}$  is the maximum braking torque expressed as multiple of the rotor torque at rated power ( $M_n$ ) and  $t_c$  the brake time constant (0.3 s). In addition, it was assumed a delay of 0.5 s between brake activation and loss of the generator torque.

$$T_b = T_b^{max} \left( 1 - e^{-\frac{t}{t_c}} \right) \quad (1)$$

The VAWT is also subject to 1 and 50 year recurrence period extreme wind conditions applying the turbulent Extreme Wind Model (EWM) during parked rotor. These situations correspond to DLCs 6.x and 7.1. The VAWT DLC 1.1 results are compared with the HAWT which is simulated in idling mode with zero and  $\pm 8$  degrees yaw misalignment according to the IEC standard. DLC 6.2 refers to loss of electrical network connection under 50 year extreme wind conditions and in this study is emulated as the case where the rotor is locked at a specific orientation therefore not able to rotate. This case could also cover the DLC 7.1 which refers to parked turbine under fault conditions with one year extreme wind assuming the fault causes the rotor to be locked at a specific azimuthal angle. DLC 6.3 refers to extreme yaw misalignment condition thus it is not relevant to VAWTs except if pitch mechanism or devices dependent on wind direction such as flaps are installed.

Table 1. Investigated design load cases.

Design situation	DLC according to IEC 61400-1 ed.3	Wind condition	Type of analysis
Power production	1.1/1.2	NTM	Ultimate and Fatigue
Power production	1.3	ETM	Ultimate
Power production	1.5	EWS	Ultimate
Power production	-	EOG	Ultimate
Power production	-	EDC	Ultimate
Emergency shut down	5.1	NTM	Ultimate
Parked-standing still and idling rotor	6.1/6.2/6.3/7.1	EWM 1 and 50 year return periods	Ultimate
Parked-idling rotor	6.4	NTM	Fatigue

## 5. Results

### 5.1. Normal power production

Simulations results of the horizontal-vertical axis wind turbines under normal power production are compared below. The mean and standard deviation (std) of the rotor torque and speed as a function of wind speed are plotted in Fig. 1 center and right, respectively. The VAWT rotor torque increases until the cut-out wind speed, in contrast to the HAWT, which after rated wind speed remains constant. This happens because the power regulation in the VAWT is done varying the rotor speed, where at high winds the rotor speed is decreased in order to confine the power output and as a result the torque increases. It is important to notice the much larger standard deviation of the rotor torque for the VAWT which is controlled only on rotor speed, while HAWT is controlled on rotor speed and blade pitching. This is inherent especially for two bladed configurations where the large variation of angle of attack during every

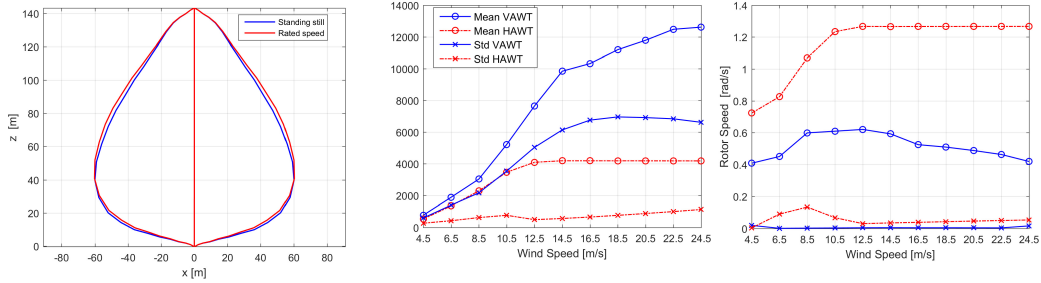


Fig. 1. VAWT rotor centreline at standing still and rated rotor speed (left). Rotor torque (centre) and rotor speed (right) as a function of wind speed for vertical and horizontal axis wind turbines.

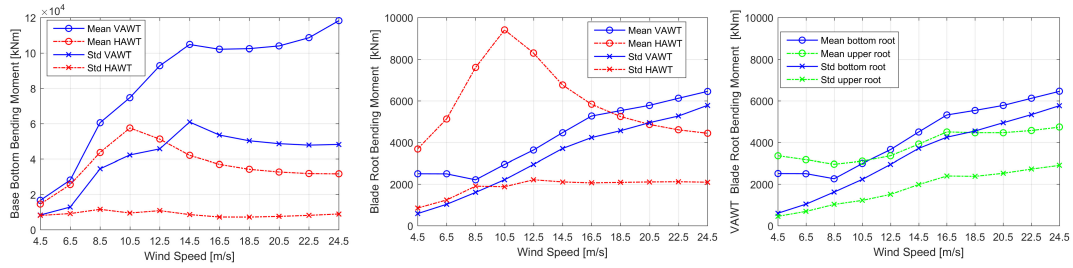


Fig. 2. Turbine base bottom bending moment (left) and blade root (low root for VAWT) bending moment (middle) as a function of wind speed for vertical and horizontal axis wind turbines. Right: Blade upper and low root bending moments as a function of wind speed for the VAWT.

revolution results in highly varied aerodynamic blade loads and causes the torque to be transmitted as a 2P loading at the generator.

The mean and std values of the turbine base bottom and blade root bending moments ( $|M_x^2 + M_y^2|$ ) for both the horizontal and vertical axis wind turbines are plotted in Fig. 2, left and middle subplots. The base bottom mean bending moment for the VAWT is close to the one of the HAWT at low wind speeds but becomes larger at high wind speeds. This is because the thrust on the NREL HAWT is decreased after reaching the rated power due to blade pitching and consequently the base bottom moments are decreased. The HAWT mean blade root bending moment is considerably higher from cut-in up to 16.5 m/s where beyond that range the values for the VAWT become significantly larger. The standard deviations are of similar magnitude up to 10.5 m/s. After that point the VAWT values are much higher while for the HAWT are almost constant but it should be recalled that the HAWT has 3 blades while the VAWT has two. The influence of centrifugal forces to the VAWT blade root bending moment at low wind speeds it is also visible, as well as the importance to run the Darrieus turbine close to the rated rotor speed in order to minimize the flapwise bending moments. Up to around 7 m/s wind speed the turbine's rotor speed is less than 0.5 rad/s, which is not close to the designed rated speed (0.62 rad/s) but at 8.5 m/s the rotor speed becomes 0.6 rad/s and the blade root bending moment decrease even though the wind speed is higher. The blade low root of the VAWT was selected for the comparison with the HAWT blade root bending moment as the loads are higher than the upper root at moderate and high wind speeds as seen in the right subplot of Fig. 2.

Next, the ultimate loads of the 50 year return period winds were computed using extrapolation of maximum values for normal operation of wind turbines under NTM wind conditions (DLC 1.1). The extrapolated loads of the turbine base bottom and blade root bending moments as a function of wind speed are given in Fig. 3 on the left and right, respectively. The extrapolation is done fitting a the Gumbel distribution [15] where the values for the extrapolation are found with the peak over threshold method. The ultimate base bottom bending moments on the VAWT are around 3.5 times higher compared to the HAWT except at low wind speeds up to 7.5 m/s. On the other the VAWT blade upper root bending moments are of similar magnitude with the HAWT blade root bending moments, while the VAWT blade low root bending moments are much larger after 10.5 m/s winds.

The equivalent 1 Hz fatigue loads under normal power production (DLC 1.2) were also computed for both wind turbines. A Wöhler exponent  $m$  equal to 3 [-] was used for the steel tower and an  $m = 10$  [-] for the composite

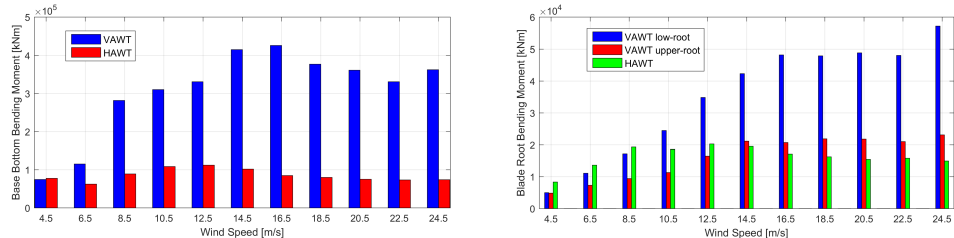


Fig. 3. Extrapolated 50 year return period extreme values of turbine base bottom bending moment (left) and blade root bending moment (right) as a function of wind speed for vertical and horizontal axis wind turbines under normal power production.

blades [16]. The equivalent 1 Hz fatigue loads for the turbine base bottom and blade root (low for the VAWT) bending moments are plotted in Fig. 4. A large difference is observed for the base bottom bending moments between the vertical and the horizontal axis wind turbines. The VAWT fatigue equivalent loads are much larger because of the cyclic aerodynamic loading for every rotor revolution. This effect is also clear in the plot of 1 Hz fatigue blade root edgewise (out of plane for VAWT) moment where after 10.5 m/s the VAWT values are much higher. The blade root flapwise (inplane for VAWT) moments are of similar magnitude for the two wind turbines. Only the VAWT low root loads are presented in Fig. 4 as their magnitude is larger compared to the upper root results.

The influence of turbulence level in the 50 year return period extreme loads (DLC 1.1) and in the 1 Hz fatigue equivalent loads (DLC 1.2) for the VAWT was conducted by simulating the three turbulence categories of the standard: A, B and C with  $I_{ref}$  equal to 0.16, 0.14 and 0.12 [-] respectively. The 50 year return period extreme blade flapwise ( $M_x$ ) and edgewise ( $M_y$ ) low root bending moments are plotted in the subplots of Fig. 5, while the subplots of Fig. 6 correspond to the 1 Hz equivalent fatigue blade low root bending moments. Both extreme and fatigue loads increase as the turbulence increases but the influence is small. The same trend was obtained from the comparison of the VAWT base bottom bending moments. It is suggested that for VAWTs two predefined turbulence categories suffice, instead of three that are proposed by the current standard.

Sensitivity analysis on the VAWT 50 year return period extreme loads (DLC 1.1) and the 1 Hz fatigue equivalent loads (DLC 1.2) for three different wind shear exponents 0.20, 0.17 and 0.14 [-] was conducted. The latter is proposed in the IEC 61400-3 standard for offshore wind turbines [6]. Both fatigue and extreme blade root and base loads were analysed and it was found that they are not affected by such changes of the wind shear. This outcome is in line with the way that the blades operate in the VAWT. A blade station remains at the same height from the ground during rotation on a given mean rotor and wind speed, while on a HAWT a blade station during every revolution confronts the wind at considerably different heights, and due to wind shear effect wind speed varies causing a 1P load contribution.

## 5.2. Ultimate loads under extreme turbulence

The IEC standard proposes the calculation of ultimate loads (50 year return period) under wind turbine normal power production by applying the ETM (DLC 1.3). The extreme turbulence standard deviation is adjusted by a parameter  $c$ . In this study the default value of  $c = 2 \text{ m/s}$  and a second value of  $c = 3 \text{ m/s}$  were used to calculate the extreme loads of DLC 1.3. The extrapolated values were always larger after 7.5 m/s wind speeds when compared

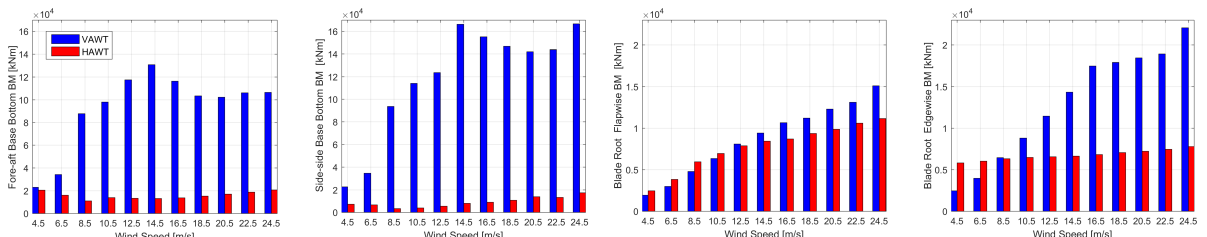


Fig. 4. Equivalent 1 Hz fatigue base bottom bending moments as a function of wind speed (first and second subplots) and equivalent 1 Hz fatigue blade root bending moments (third and forth subplots) under normal power production.

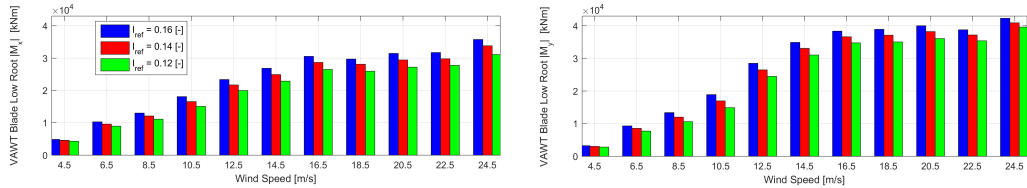


Fig. 5. Influence of turbulence intensity in the extrapolated 50 year return period extreme VAWT blade low root bending moments under normal power production.

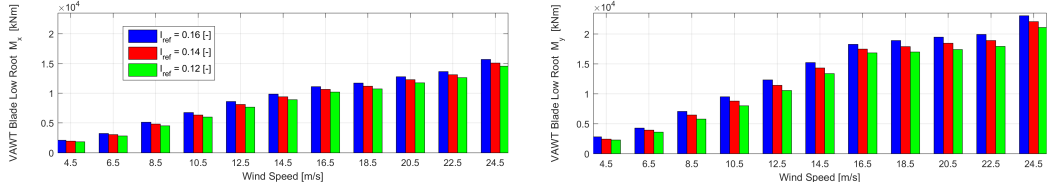


Fig. 6. Influence of turbulence intensity in the equivalent 1 Hz fatigue VAWT blade low root bending moments under normal power production.

with the results from DLC 1.3 even with the increased  $c$  factor. This holds for the base bottom and blade low root bending moments. It can be said that this model is calibrated for HAWTs to give the extreme values in a simpler way than the extrapolation method of DLC 1.1 and should be checked further for the case of VAWTs.

### 5.3. Extreme wind shear

An extreme event that is proposed by the standard as potentially critical during the normal operation of the wind turbine is the transient extreme wind shear (EWS), which corresponds to DLC 1.5. It refers to vertical and horizontal wind shear (wind veer) and can be positive or negative. The duration of the extreme event was kept to the default value of 12 s. The maximum base bottom and blade low root bending moments emerging from the extreme wind shear and wind veer transient events are lower throughout the operational wind speed range when are compared with the DLC 1.1 results. The results agree with the sensitivity analysis that presented above regarding the effect of wind shear to the loads and can be concluded that the extreme wind shear event is not a critical DLC for the VAWT.

### 5.4. Extreme operating gust

Simulations of EOG were performed at 8.5, 14.5, 18.5 and 24.5 m/s wind speeds. In Fig. 7 are plotted the time series of the VAWT blade-1 low root flapwise (left subplots) and edgewise (right subplots) moments where the gust passes through the rotor plane at three different time stamps as shown at the first 3 rows of subplots. The wind speed before and after the transient event is 14.5 m/s in this case. It can be seen that the maximum emerging loads are dependent on the rotor orientation and the time where the frontal passage of gust goes through the rotor plane. Relevant results were obtained for the VAWT base bottom bending moments and the rotor torque while the rotor speed changes slightly due to the large inertia of the rotor. The 3D extension of the rotor in space results in a relatively low load increase. Interpretation of the results revealed that the VAWT EOG simulations should cover different rotor orientations and then the largest load should be considered. The maximum loads for both the base bottom and blade root bending moments were found when the gust was applied on top of a 24.5 m/s mean wind speed.

### 5.5. Extreme wind direction change

Simulations were conducted for every wind speed bin from cut-in up to cut-out, considering positive as well as negative extreme wind direction change with the VAWT under normal power production. The EDC event was applied as described in the standard. The magnitude of the velocity vector during the wind direction change remains the same and only the velocity components in x and y direction alter magnitudes. The ultimate loads emerged from the EDC event are lower when compared with the ultimate loads of DLC 1.1. Since the VAWT rotor is omnidirectional the result is almost unaffected from the quick change in wind direction in contrast to a HAWT.

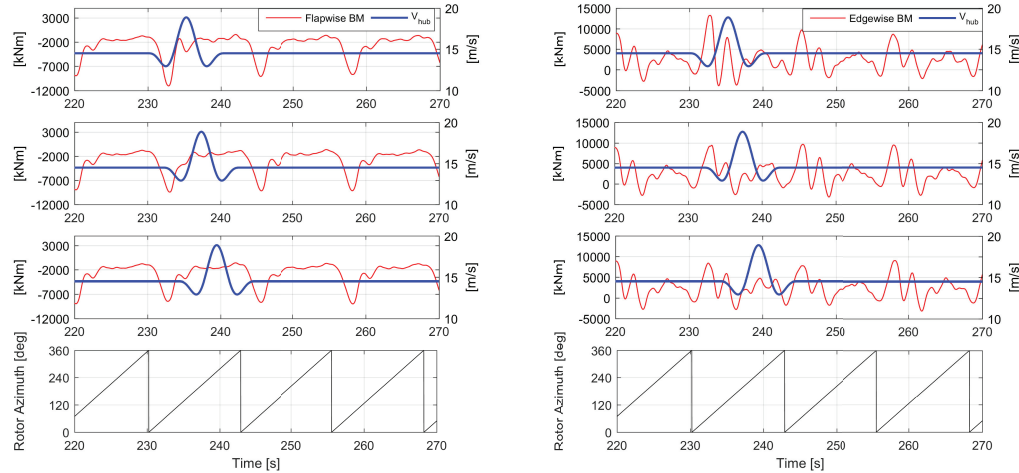


Fig. 7. Time series of VAWT blade-1 low root bending moments  $M_x$  (left subplots) and  $M_y$  (right subplots) during the EOG event at 14.5 m/s. The gust frontal passage passes the rotor plane at 3 different time stamps (corresponding to different rotor orientations), each one represented at the 1<sup>st</sup>, 2<sup>nd</sup> and 3<sup>rd</sup> row of sub-plots.

### 5.6. Emergency shut down

In Fig. 8 are plotted the VAWT blade low root bending moments (upper left subplot), the blade station positions x and y at equator height (upper right subplot), the rotor azimuth angle and speed (lower left subplot) and the rotor and brake torque (lower right subplot) for an emergency wind turbine shut down. The wind turbine operates at 14.5 m/s wind speed and at 220 s simulation time the mechanical brake is activated. The generator is deactivated half second before, corresponding to a grid loss situation, therefore the rotor accelerates for a short period as it can be seen in the lower left subplot. In this simulation the maximum brake torque is set to  $3 M_n$  and the brake time constant  $t_c$  to 0.3 s. The turbine decelerates to the rotor speed of 10% of rated within 9 s from the moment of brake activation (6 s are needed if  $T_b^{max} = 4M_n$ ). Regarding the turbine base bottom no peak loads were seen during the first seconds of the brake activation, but there was a small fluctuation of the loads even after 50 s of the brake event due to the dynamics of the rotor. Similar behaviour is observed for the blade low root bending moments, as for the turbine base bottom, except that the fluctuation of loads after the first 10 s is more dominant for the out of plane ( $M_y$ ) bending moment. The relative blade station motion at equator height reveals that the blade does not deform more during the deceleration phase. The above brake configuration and wind condition simulation results revealed that the turbine base and blade ultimate loads are not extreme during the emergency stop. Sensitivity analysis of the maximum loads for the turbine base bottom and blade roots for different wind speeds and brake parameters was conducted. The maximum base bottom moments in general increase as the brake time constant increases, while for the maximum blade root moments the correlation is opposite. In addition, the loads emerging from the different brake torques are almost the same for the turbine base bottom but for the blade roots the loads increase as the maximum brake torque increases. The overall maximum blade and base loads emerged from the simulations at 24.5 m/s wind speed condition.

### 5.7. Parked rotor

The VAWT was firstly simulated applying the 50 year extreme wind speed and assuming that the rotor is idling without any generator torque. Under these conditions the rotor constantly accelerates beyond rated rotor speed without reaching any equilibrium point as in HAWT with 90 degrees pitched blades. Thus the rotor was forced to rotate at 5% and 10% of rated rotor speed. This scenario is interpreted as DLC 6.1 for the VAWT. The loads were compared with the HAWT in idling mode with 90° pitch angle and yaw misalignments of 0° and 8° under the same environmental conditions. The most important results are summarized in Table 2. The VAWT base bottom and blade root bending moments are higher compared with the HAWT with or without yaw misalignment results. The maximum loads and deflections emerging for the two simulation scenarios of the VAWT are very close.

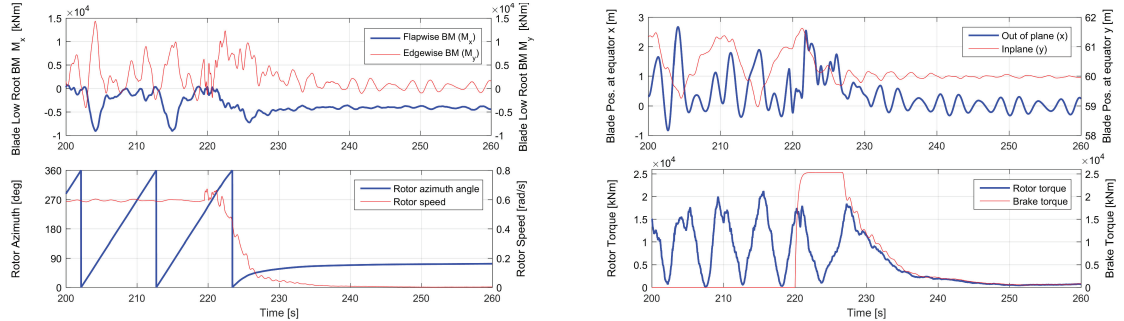


Fig. 8. Time series of the VAWT blade low root bending moments (upper left), the blade station position x, y at equator height (upper right), the rotor azimuth angle (lower left) and rotor speed (lower right) during emergency shut down ( $t_c = 0.3$  s,  $T_b^{max} = 3M_h$ ).

Table 2. Loads and deflections under 50 year recurrence period wind conditions with forced rotor speed for VAWT and idling for HAWT.

Maximum absolute values	VAWT		HAWT	
	forced rotor speed % of rated		Yaw misalignment in degrees	
	5	10	0	8
Base bottom BM $ M_x^2 + M_y^2 $	[kNm]	$30.5 \times 10^4$	$29.8 \times 10^4$	$6.2 \times 10^4$
Rotor torque	[kNm]	$2.2 \times 10^4$	$2.4 \times 10^4$	$0.6 \times 10^4$
Blade low root BM $ M_x^2 + M_y^2 $	[kNm]	$2.6 \times 10^4$	$2.7 \times 10^4$	-
Blade upper root BM $ M_x^2 + M_y^2 $	[kNm]	$1.8 \times 10^4$	$1.8 \times 10^4$	-
Blade root BM $ M_x^2 + M_y^2 $	[kNm]	-	-	$0.6 \times 10^4$
Blade deflection x at equator height	[m]	3.7	3.6	-
Blade deflection y at equator height	[m]	3.5	3.6	-
Blade deflection z at equator height	[m]	3.6	4.0	-

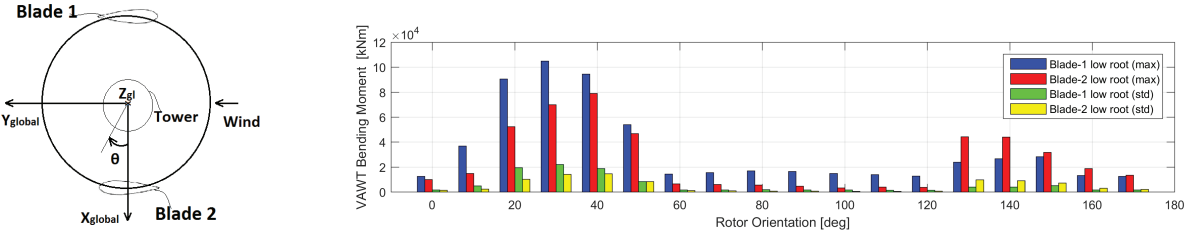


Fig. 9. Parked and locked VAWT rotor at different orientations exerted to 50 year recurrence period extreme winds. Left: Rotor cross-section at equator height, depicting the orientation of the blades. Right: Maximum and standard deviation of blade 1 and 2 low root bending moments.

DLC 6.2 was investigated as described in the design load cases section assuming that the VAWT rotor is parked and locked at different orientations under the 50 year recurrence period wind. The simulations were performed from azimuthal angles  $\theta = 0^\circ$  to  $170^\circ$  with a step of  $10^\circ$ . The ultimate blade low root bending moments are given in Fig. 9. When the rotor orientation is not close to  $0^\circ$  and  $90^\circ$  (or equivalently  $180^\circ$  and  $270^\circ$ ) an abrupt increment in loads exists. Blade oscillation was detected in these orientations which built up when the time series of blade deformation were screened. Further simulations were performed without turbulence at the same wind speed and setting all the components totally stiff, except the blades. High blade root loads and blade oscillation were found at the same regions of rotor orientation as before. Sensitivity analysis of the standing still case was conducted by increasing the blade stiffness 50% and 100% separately each time and the logarithmic damping decrement of the first blade mode from 3% to 5%. The results show that the instabilities are present in the same rotor orientations as described above. The long blades in combination with the absence of stiffening effects from centrifugal forces in standing-still mode could be considered the primary reasons that lead to blade instability. From the findings the standing still locked rotor under extreme wind condition appears to be critical design driver for large scale Darrieus VAWTs. However these findings must be considered to be quite uncertain as the aerodynamics may not be fully valid in this particular situation.

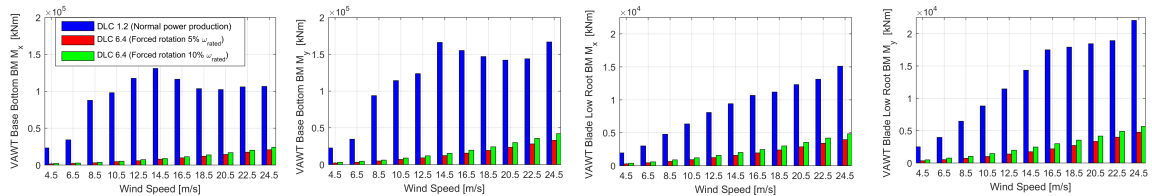


Fig. 10. VAWT equivalent 1 Hz fatigue base bottom bending moments  $M_x$  and  $M_y$  as a function of wind speed (first and second subplots) and equivalent 1 Hz fatigue blade root bending moments  $M_x$  and  $M_y$  (third and forth subplots) comparison of DLC 1.2 and DLC 6.4.

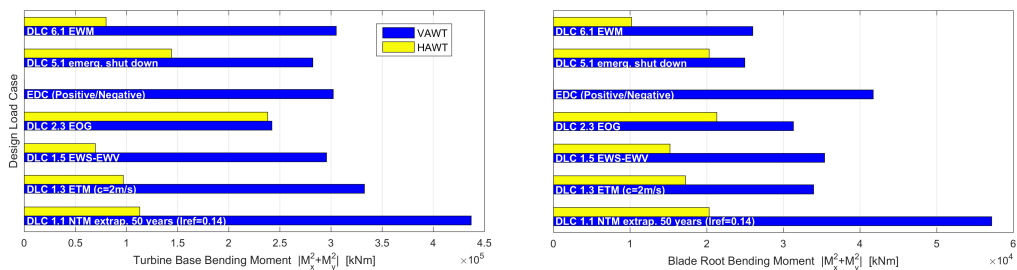


Fig. 11. Comparison of the VAWT DLCs absolute maximum bending moments at the turbine base (left) and the blade root section (right).

The VAWT 1 Hz equivalent fatigue loads were extracted for the same forced rotor speeds as the ultimate load analysis above (5% and 10% of rated) and compared with the one of normal power production (DLC 1.2). This case corresponds to DLC 6.4 of the standard and is considered relevant for the VAWTs too.

In Fig. 10 the equivalent 1 Hz fatigue loads for the turbine base bottom and blade low root bending moments  $M_x$  and  $M_y$  are plotted. The loads arising from the forced rotation mode are considerably lower in comparison with the normal power production equivalent loads for both the blade low root and the turbine base bottom. A small difference in loads can be seen between the two different forced rotor speeds, while the loads increasing as the wind speed increases.

The absolute maximum bending moments from each DLC for VAWT and HAWT base bottom and blade root (low root for the VAWT) are compared in Fig. 11. The results from DLC 6.2 are not included since blade instability occurred for VAWT resulting to very high loads. The loads emerging from DLC 1.1 are the highest for both and follow the loads from the DLC 1.3 for the turbine base bottom and the positive EDC for the blade roots. From the investigated extreme transient events (EDC, EOG, EWS, EWV) and emergency shut down the VAWT maximum loads always emerge at maximum operational wind speed rather than rated. For the HAWT DLC 6.1 and DLC 6.2 return the highest loads for the tower bottom and blade root.

## 6. Conclusions

The IEC 61400-1 ed.3 standard was studied regarding its applicability for VAWTs based on HAWC2 simulations of a 5 MW 2-bladed Darrieus rotor. Many DLCs were investigated and a comparison of load levels with a similar nominal power HAWT was conducted. To a large degree the current DLCs are applicable to VAWTs but some of them appear redundant and others need to be modified. The definition of hub height was clarified for the VAWT rotor. EWS and EWV transient wind conditions are not critical in terms of loading of the VAWT structure.

The VAWT maximum loads always emerge at maximum operational wind speed rather than rated for the investigated extreme transient events (EDC, EOG, EWS, EWV). Extreme operating gust wind condition simulations revealed that the emerging loads depend on the rotor orientation when the frontal passage of gust passes through the rotor. As a result, the application of EOG should be investigated in combination with different rotor orientations due to the 3D extension of the rotor in space. Transient change in wind shear and extreme direction change cases were not followed by large transient loads in the VAWT simulations. The VAWT loads arising from the emergency shut down scenario were lower compared with the statistical extrapolated 50 year return period loads of DLC 1.1 when the brake torque is

set equal to 3 and 4 times the generator torque at nominal rotor speed. The interpretation and simulation of DLC 6.2 in this study led to blade instabilities. Further investigations are suggested to confirm if this can appear in a real turbine.

From the load comparison between the vertical and the horizontal axis wind turbines was found that the maximum and the equivalent 1 Hz fatigue base bottom bending moments of vertical axis turbine are much higher compared with the HAWT equivalent under normal power production. On the other, the blade root maximum and 1 Hz fatigue loads between the two concepts are of similar magnitude for low and moderate wind speeds. DLC 1.1 simulations returned the highest tower bottom and blade root loads for the VAWT where DLC 2.3 for the HAWT.

## Acknowledgements

The present work is a result of the contributions within the INFLOW project, supported by the European Commission, Grant No 296043, and by the INFLOW beneficiaries: NENUPHAR(F), IFP(F), EDF(F), EIFAGE(F), FRAUNHOFER(D), VICINAY(E), VRYHOF(NL), and DTU(DK).

## References

- [1] International Electrotechnical Commission (IEC). Wind turbines Part 1: Design requirements, IEC 61400-1, 3rd edition. IEC. Switzerland, 2005.
- [2] Larsen TJ, Hansen AM, How 2 HAWC2, the user's manual. DTU Wind Energy, Technical Report R-1597(ver. 4-5)(EN). Roskilde, Denmark, 2014.
- [3] Madsen HA, Larsen TJ, Vita L, Paulsen US. Implementation of the Actuator Cylinder flow model in the HAWC2 code for aeroelastic simulations on Vertical Axis Wind Turbines. In 51st AIAA Aerospace Sciences Meeting including the New Horizons Forum and Aerospace Exposition, 2013.
- [4] Verelst DR, Madsen HA, Kragh KA, Belloni F. Detailed Load Analysis of the baseline 5MW DeepWind Concept. DTU Wind Energy, Technical Report E-0057. Roskilde, Denmark, 2009.
- [5] Jonkman JM, Butterfield S, Musial W, Scott G. Definition of a 5 MW Reference Wind Turbine for Offshore System Development. National Renewable Energy Laboratory, Technical Report NREL/TP-500-38060. Golden, Colorado US, 2009.
- [6] International Electrotechnical Commission (IEC). Wind turbines Part 3: Design requirements for offshore wind turbines, IEC 61400-3. IEC. Switzerland, 2005.
- [7] Galinos C, Study of Design Load Cases for Multi-Megawatt Onshore Vertical Axis Wind Turbines. European Wind Energy Master Thesis. Roskilde, Denmark, 2015.
- [8] Øye S, Dynamic stall-simulated as time lag of separation. In Proceedings of the 4th IEA Symposium on the aerodynamics of wind turbines, 1991.
- [9] Hansen MH, Gaunaa M, Madsen HA. A Beddoes-Leishmann type dynamic stall model in state-space and indicial formulations. Risø National Laboratory, Technical Report R-1354(EN). Roskilde, Denmark, 2004.
- [10] Larsen TJ, Madsen HA. On the way to reliable aeroelastic load simulation on VAWT's. In Proceedings of EWEA, 2013.
- [11] Larsen TJ, Madsen HA, Larsen, GC, Hansen, KS. Validation of the dynamic wake meander model for loads and power production in the Egmond aan Zee wind farm. Wind Energy, 16(4), 605624, 2013.
- [12] Galinos C, Aeroelastic study of Vertical Axis Wind Turbine based on Sandia 500 kW test-bed. Special Project report. Roskilde, Denmark, 2015.
- [13] Madsen HA, Larsen TJ, Vita L, Paulsen US. Implementation of the Actuator Cylinder flow model in the HAWC2 code for aeroelastic simulations on Vertical Axis Wind Turbines. In 51st AIAA Aerospace Sciences Meeting including the New Horizons Forum and Aerospace Exposition, 2013.
- [14] Larsen TJ. Slip generator model implemented in HAWC2 as an external DLL. Risø Technical Note 200500523, Roskilde, Denmark, 2005.
- [15] Moriarty PJ, Holley WE, and Butterfield SP, Effect of turbulence variation on extreme loads prediction for wind turbines, Journal of Solar Energy Engineering, Asme 124(4), 387395, 2002.
- [16] Brnødsted P, Lilholt H, and Lystrup A, Composite Materials for Wind Power Turbine Blades. Annual Review of Materials Research, 35:505-538, 2005.